Hybrid sol-gel coatings for reducing wettability and storage degradation of biomass pellets

Cutz, Luis; Tiringer, Urša; de Jong, Wiebren; Mol, Arjan

DOI
10.1016/j.matchemphys.2023.127861

Publication date
2023

Document Version
Final published version

Published in
Materials Chemistry and Physics

Materials Chemistry and Physics 304 (2023) 127861

Contents lists available at ScienceDirect

Materials Chemistry and Physics

journal homepage: www.elsevier.com/locate/matchemphys

Hybrid sol-gel coatings for reducing wettability and storage degradation of biomass pellets

Luis Cutz [a,*,1], Urša Tiringer [b,1], Wiebren de Jong [a], Arjan Mol [b]

[a] Section of Large-Scale Energy Storage (LSE), Department of Process & Energy, Faculty of Mechanical, Maritime and Materials Engineering, Delft University of Technology, Delft, the Netherlands

[b] Section of Corrosion Technology and Electrochemistry, Department of Materials Science and Engineering, Faculty of Mechanical, Maritime and Materials Engineering, Delft University of Technology, Delft, the Netherlands

HIGHLIGHTS

- GPTMS/TEOS sol-gel is compatible with the heterogenous composition of biomass pellets.
- The coating offers a sealing function reducing the mean apparent depth of the cracks.
- After 1 month of storage, the coated pellets retained their hydrophobic behavior.

ARTICLE INFO

Keywords:
Biomass pellets
Hydrophobic coating
Durability
Storage
Biomass treatment

ABSTRACT

Long transport distances and extended storage of biomass pellets especially in humid environments provide a suitable setting for enhanced degradation in the form of moisture sorption, cracking and attrition. We developed an optically transparent, low-cost and environmentally friendly coating to reduce moisture sorption and storage degradation of pellets. The developed coating is a hybrid sol–gel, based on tetraethoxysilane (TEOS) and 3-glycidoxypropyl-trimethoxysilane (GPTMS) precursors. We coated two types of untreated and one type of torrefied wood pellets and stored them in a climate chamber during 1 month simulating a ship's hold, at a constant condition of 40 °C and 85% relative humidity. After 1 month of storage, the mean water contact angle increased by a factor of two compared to the uncoated ones. The lower wettability of the sol-gel coated untreated pellets compared to the non-coated torrefied pellets might provide an alternative to torrefaction.

1. Introduction

The current biomass demand, promoted by climate targets and sustainable development goals, has exposed the weaknesses of local biomass supply chains, boosting the international trade of pellets [1]. One third of the global consumption of pellets in 2018 required transhipment, from the Americas to Europe and Asia [1]. Thus, depending on the transportation distance and type, pellet storage can range from days to months [2,3]. During transport, handling and storage, pellets face fluctuating environmental conditions such as high temperatures and high relative humidity which most often results in moisture sorption leading to cracking, (increased) bacterial and/or fungal activity and particle breakage, referred to as storage degradation [3,4]. The combination of these degradative phenomena results in reduced mechanical durability, reduced heating value, self-heating and spontaneous combustion of pellets [3,5–8]. Storage degradation in the form of pellet breakage also generates dust particles which can lead to equipment fouling and risks to workers' health from exposure to dust [5,7,9]. The transition from fossil to renewable resources will demand more attention and regulation in the quality of these products.

Various approaches have been developed to improve the resistance of pellets to storage degradation such as inorganic/organic based additives or coatings [10–12] and thermal pre-treatments [13]. Yet, even the most recent thermal pretreatments such as torrefaction, have not addressed storage degradation effectively [4,14,15]. Although protection of materials is an ancient topic, it wasn't until the Industrial Revolution that this topic experienced a substantial change into a highly advanced and technological field [16]. As industrial sectors matured,

* Corresponding author.
E-mail address: luis.cutz@tudelft.nl (L. Cutz).
[1] These authors have equally contributed to this work.

https://doi.org/10.1016/j.matchemphys.2023.127861
Received 30 December 2022; Received in revised form 12 April 2023; Accepted 30 April 2023
Available online 9 May 2023

their quest for high quality products made them research and develop the first generation of protective coatings [16]. Coatings nowadays are extensively used in the automotive and aircraft industry, among others [17,18]. Thus, we foresee that as other sectors have incorporated protective coatings to preserve the quality of their products and comply with stricter regulation, the bioenergy sector will follow the same path. Few developments are found in literature regarding coatings to minimize moisture sorption or to lower the rate of storage degradation of biomass pellets. The most recent studies include the use of mineral and vegetable oil-based coatings [19] or commercial coating agents dissolved in isopropyl alcohol [20] to improve the hydrophobicity of pellets at ambient temperature with RH $\leq$ 60%. The findings of these studies highlight the benefits of using coatings to produce moisture resistant biomass pellets. Nonetheless, one of the weaknesses of additives such as isopropyl alcohol is that this evaporates at ambient temperature [20], which could represent a risk in enclosed storage due to increased concentration of this gas. Furthermore, questions regarding the sustainability of these coatings and their tolerance to high humidity environments during extended storage remain unanswered. The closest application regarding the use of coatings to protect organic materials is found in wood surfaces. Coatings have been extensively researched with the aim of improving the properties of wood surfaces exposed to humid conditions, yielding efficient protection [21,22]. Among them, hybrid sol-gel coatings are promising materials to decrease the rate of moisture uptake, enhance fire-resistance properties and mitigate discoloration of wood [23–26]. They are also known for their cost affordability [27,28], facile application, controlled porosity and hydrophobicity [29,30]. They are synthetized by the sol-gel process, which is classified as a "green" technology since it uses compounds that do not introduce impurities into the end product, is waste-free, excludes the stage of washing and requires low processing temperature, providing substantial energy savings [31]. Another advantage of the sol-gel process is that in some applications, the sol-gel process is now more economically viable than other coating techniques thanks to recent improvements in its economics [28]. For instance, compared to other coating techniques, the sol-gel process often uses low-cost precursors [32] and low-to-moderate cost equipment for deposition of the coating compared to conventional methods [33]. Furthermore, sol-gel coatings can be used in thin layers, which saves material costs [34]. Moreover, sol-gel coatings have great adhesion and toughness, which can result in coatings that last longer over time and require less care [34]. Although sol-gel coatings are effective on wood surfaces [35], it is known that biomass pellets have different physicochemical properties and morphological features. For example, wood surfaces are known to have a uniform surface [36] and a more homogeneous composition compared to biomass pellets, which are known to have a highly heterogeneous composition, high fibrous nature, surface cracks, inorganic-based inclusions and regions with fiber ends [4]. The differences between these two material types are significant. Thus, in the present work, we aim to study the compatibility of a hybrid-sol gel with biomass pellets to reduce moisture sorption and withstand long term storage.

The basic principle of the hybrid sol-gel process usually involves polycondensation reactions between inorganic metal alkoxides ($M(OR)_4$) and organic alkoxides ($M(OR)_3R'$)), where M represents a metal, R an alkyl group and R' an organic functional group, such as methacryloyl, epoxy or styryl [37,38].

Among the inorganic alkoxides, alkoxysilanes (e.g., tetraethoxysilane - TEOS) are the most widely used for sol-gel applications [39–42]. When reacting with wood, alkoxysilanes can easily penetrate the middle lamellae and interior of wood cells because of wood's porosity. Part of the alkoxysilanes that penetrates the wood cells precipitates as silica polymers, which act as fillers that enhance the physical and mechanical properties of the wood matrix [30]. The other part of alkoxysilanes undergo two different chemical reactions when in contact with wood [43,44] due to the presence of hydroxyl groups in wood. The first reaction binds the alkoxide hydroxyl groups to the free hydroxyl groups of wood via hydrogen bonds. The second reaction is the condensation between silanol and the hydroxyl groups of wood, which connects the wood and silica via Si–O–C bonding structures [45,46].

When the goal is to increase wettability, alkoxysilanes are rarely used on their own. This is due to the hydroxyl groups ($Si(OH)_4$) in alkoxysilanes resulting from the hydrolysis process provide coatings with a hydrophilic nature. Thus, hybrid sol-gel coatings are typically mixed with organic alkoxysilane precursors [28,38,47–49] such as 3-glycidoxypropyltrimethoxysilane (GPTMS). When in contact with wood, the epoxy ring of GPTMS reacts with the hydroxyl groups of the cellulose fibre and graft on the fibre surface [50,51], increasing the hydrophobicity of wood [30,38].

In order to understand the hydrophobic behavior of hybrid sol-gels when deposited on biomass, we coated two types of untreated and one type of torrefied wood pellets with a hybrid sol-gel based on TEOS/GPTMS precursors. This type of coating is one among the realm of hybrid sol-gel coatings but as far as the authors are aware, this is the first-time a GPTMS/TEOS hybrid sol-gel coating is applied to biomass pellets. Our coating is applied using a dip-coating technique, which is a low-cost and high-efficiency method, widely applied in industry [34]. Furthermore, to test the resistance of the coating to storage degradation we stored the coated pellets in a climate chamber during a period of 1 month at a constant temperature of 40 °C and relative humidity of 85%. We characterized the uncoated and coated pellets before and after storage, using the following techniques: gravimetric analysis (weight-loss-test), digital microscopy, scanning electron microscopy equipped with energy dispersive X-ray spectroscopy (SEM-EDS), thermogravimetric analysis (TGA), Fourier-transform infrared spectroscopy (FTIR) and water contact angles measurements (optical tensiometer). The combination of these techniques provides a more comprehensive understanding of the effectiveness of the GPTMS/TEOS hybrid sol-gel coating in protecting pellets from moisture and storage degradation. Our method offers a new approach towards the development of sustainable and cost-competitive coatings to preserve the quality of biomass pellets. These advantages may result in lower transportation, storage, and product loss during handling.

2. Materials and methods

2.1. Materials

We monitored two types of untreated commercial white wood pellets, wood pellet type I (wp1) and wood pellet type II (wp2), and one type of torrefied pellets (tor). On average, the studied pellets measure 6 mm in diameter and 3 cm in length [7]. The elemental analysis of the samples is provided in the E-supplementary data. Wood pellets were made from sawdust and purchased from local stores in the Netherlands. No information was available regarding the manufacturing process. The torrefied pellets were obtained from a pilot plant in the UK and no information was provided about the origin of the pellets and production process.

2.2. Sol-gel synthesis and preparation of coated pellets

The hybrid sol-gel was prepared by mixing TEOS (Aldrich, 99%), GPTMS (ABCR, 98%) and colloidal silica SiO_2 (Ludox-4S, Aldrich, aqueous suspension 40 wt%). SiO_2 nanoparticles were added to the formulation to decrease the porosity of the coating and increase its thickness [52]. After 30 min of stirring, 0.6 mL of concentrated HNO_3 (VWR, 65%) was added as a catalyst for polycondensation. Finally, absolute ethanol (EtOH, Panreac, 99.8%) was added as a solvent. The molar ratio of the hybrid sol-gel (SG) was $TEOS/GPTMS/SiO_2$ = 0.40/0.46/0.14. SG was deposited on wp1, wp2 and tor using a dip-coating technique, with a withdrawal rate of 30 cm/min. This withdrawal rate has proved to deliver a homogeneous coating using a dip-coating technique on different types of surfaces [53,54]. Coated

samples were thermally treated in an oven (Binder 2.0) for 1 h at 120 °C to complete the polymerization between SG and pellet. The oven temperature was programmed from room temperature to 120 °C using a heating rate of 5 °C/min.

2.3. Storage conditions

Uncoated and coated pellets were stored in a climate chamber (C+10/600 Climate Test Chamber) with a volume of 600 L for a period of 1 month at a constant temperature of 40 °C and 85% RH. These conditions represent typical conditions of a ship's hold during a trans-atlantic journey [7,55,56]. During the storage period, we examined the pellets at three sample dates: day 0, after 10 days and after 1 month. To rule out any possible interaction between the biomass components and the coating, we tested the reduction of the coating layer separately by storing the hybrid sol-gel coating under the same conditions (40 °C and 85% RH).

2.4. Characterization techniques

Weight and diameter of pellets: The pellet weight and diameter of the uncoated pellets were characterized according to EN standard 16127. The weight of the coating and coated pellets was measured using an electronic balance (Sartorius Practum 124-1S analytical). The diameter of the coated samples was measured crosswise with a Kunzer 7EMS01 digital caliper 150 mm with an accuracy of 0.01 mm. The changes in diameter and weight (Δx) are calculated based on Eq. (1):

$$\Delta x = \frac{x_2 - x_1}{x_1} \quad (1)$$

Where x_1 and x_2 is the weight/diameter of the samples before and after storage, respectively. The weight change represented by Eq. (1) is also known as the equilibrium moisture content (EMC).

Thermogravimetric analysis (TGA) and differential scanning calorimetry (DSC) of sol-gel: A thermogravimetric analyser (TGA, Thermal Advantage SDT Q600) was used to measure the combustion behavior of the sol-gel solution. The samples (initial weight ≅ 17 mg) were placed in an alumina cup and heated from room temperature to 1000 °C at a heating rate of 10 °C/min under an air flow of 50 mL/min.

Fourier-transform infrared spectroscopy (FTIR) of sol-gel: The functional groups in the GPTMS/TEOS hybrid sol-gel solution were identified by FTIR. The FTIR spectrum of a droplet of sol-gel solution was recorded between 4000 cm^{-1} and 700 cm^{-1}, using a PerkinElmer Spectrum 100 spectrometer in attenuated total reflectance (ATR) operation mode. The spectrum is presented as absorbance [%].

Digital microscopy: We used digital microscopy to examine the penetration of the coating into the pellet and to monitor any potential coating degradation during storage. The penetration of the coating is assumed to be related with the apparent crack depth at the surface of the pellet. The apparent depth of surface cracks was determined using a built-in tool in the microscope software to create a 3D profile measurement of the side of the pellet facing the microscope objective [57]. A 3D profile is created by drawing a line along the longest axis of the front face of the sample. The profile represents the depth distribution along the surface line, where the central region of the crack is identified by a peak compared to the flat non-cracked surface. A total of 6 samples (i.e., two samples per type of pellet) were analysed before coating and after coating using a digital microscope Keyence VHX-5000 series, ocular VH-Z100 R/W/T. To ensure repeatability, we drew three 3D profile lines along the front face of each sample. The apparent depth of each type of pellet (tor, wp1 and wp2) is reported as the average of the two samples.

Wettability: The wettability of the pellets was defined by the contact angle between a water droplet and the pellet's surface. We measured the water contact angle of 6 samples (i.e., two samples per type of pellet) before coating and after coating, at the three sample dates using an Easy Drop Standard system Kruss DSA 100 equipment. Six measurements were performed on different areas of each sample. The mean water contact angle of each type of pellet (tor, wp1 and wp2) is reported as the average of the two samples.

Scanning electron microscopy and Energy dispersive spectroscopy (SEM-EDS): The morphology and elemental composition of the coated pellets' surfaces were analysed using SEM-EDS across the three sample dates. SEM analysis was performed on a JEOL IT100 microscope using a backscattered electron detector, coupled with an energy dispersive spectrometer. EDS measurements were carried out at low-vacuum due to the non-conductivity of the samples. SEM images were recorded in a compositional mode using an accelerated voltage of 10 kV and probe current of 65 pA. We analysed one sample per each type of pellet. Each pellet was glued to the sample holder using double-sided sticky tape. SEM-EDS analysis was carried out at 2 different regions of interest (ROI) per sample. EDS mapping was performed at each ROI and in average, we selected 4 points per each ROI for scanning. All samples were returned to the climate chamber once the SEM-EDS analysis was performed. The data was processed using the InTouchScope™ software. Detailed information on the morphology of the uncoated pellets can be found in Ref. [4].

3. Results and discussion

3.1. Weight and diameter change

The changes in diameter and EMC of the uncoated and coated pellets after 1 month of storage are presented in Fig. 1. These two variables are an indicator of the resistance of the coating and hydrophobicity of pellets. Higher diameter change (%) means increased swelling of the pellet and reduced protection by the coating, while a higher EMC suggests reduction of the coating layer and increased hygroscopicity of the coated pellets. Data for the uncoated pellets (Fig. 1) after 1 month of storage was extracted from Ref. [4].

After 1 month of storage, the coating reduced the swelling of the pellets compared to the uncoated ones, especially for wp2. The wp1 pellet is the most porous one and is thus more prone to adsorb moisture from the environment compared to tor and wp2. This has been confirmed by micro-CT measurements reported in our previous study on pellet degradation [4]. As can be seen from Fig. 1, the EMC of the uncoated torrefied pellets after 1 month of storage is comparable to the values obtained for the uncoated wp1 and wp2. Nonetheless, depending on the type of biomass and operational conditions, torrefaction is known to significantly increase the hydrophobic behavior of pellets compared to raw untreated biomass [58,59]. Zhang et al. [59] observed that torrefied pine wood pellets stored in a controlled environment (22−23 °C and 48−52% RH) for up to 18h decreased the EMC by 70% compared to raw untreated biomass. Meanwhile, our results indicate that the coated pellets, untreated or torrefied, lost weight gradually (Fig. 1) during 1 month of storage, which indicates no sign of moisture sorption and suggest degradation of the coating via evaporation. This is backed up by measurements of the weight of the coating alone after 1 month of storage, which indicate that the average weight of the coating alone decreased by 0.7% compared to the initial weight prior to storage. Thus, it appears that the reduced EMC is related to the composition of the GPTMS/TEOS hybrid sol-gel and stability of the coating at high storage temperatures (40 °C) and high relative humidity (85% RH). Meanwhile the swelling of the pellets is related to moisture sorption and off-gassing [60]. Thus, our findings suggest that there is a competition between coating stability and moisture sorption which will govern the rate of pellet degradation.

3.2. TGA analysis

Fig. 2 presents the TGA and DSC thermograms of the sol-gel. The sol-gel was thermally degraded between room temperature (17 °C) and

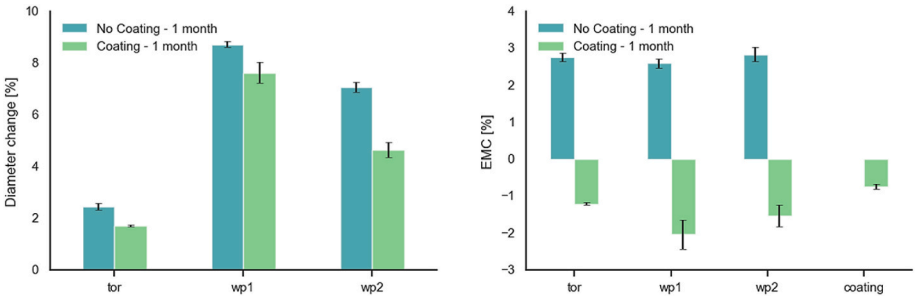

Fig. 1. Changes in diameter and weight of coated biomass pellets and coating after 1 month after storage. Data for the uncoated pellets after 1 month of storage was extracted from Ref. [4].

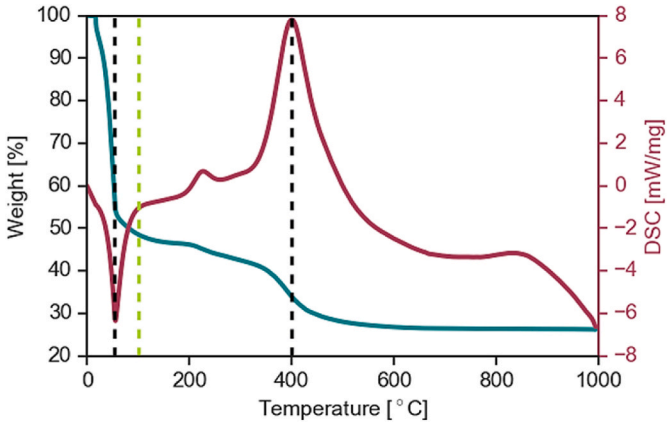

Fig. 2. TGA and DSC curves of the GPTMS/TEOS hybrid sol-gel. The blue-green line represents weight [%] and red-magenta line indicates the DSC curve [mW/mg]. The first inflection point (53 °C, black dashed line) was determined by calculating the maximum gradient of the TGA curve. The lime-green dashed line indicates 100 °C. The second inflection point (400 °C, black dashed line) was obtained from the peak of the DSC curve. (For interpretation of the references to color in this figure legend, the reader is referred to the Web version of this article.)

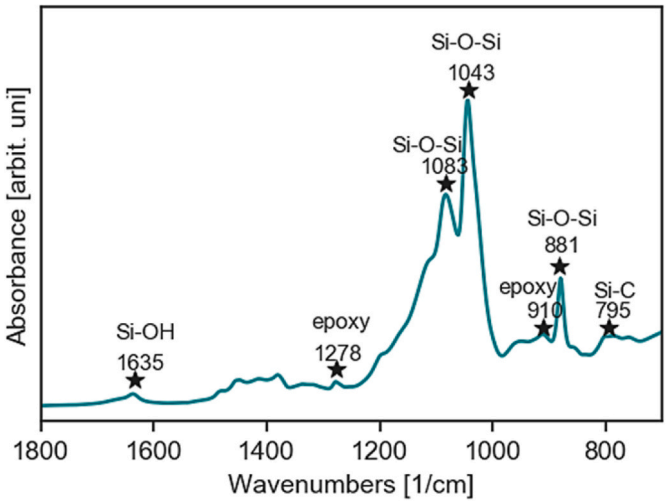

Fig. 3. FTIR spectrum of the GPTMS/TEOS hybrid sol-gel. The blue-green line represents the absorbance spectrum and the stars indicate the position of peaks in the spectrum. (For interpretation of the references to color in this figure legend, the reader is referred to the Web version of this article.)

1000 °C. These results provide preliminary information on the stability of the sol-gel coating during subsequent thermochemical conversion or combustion.

The decomposition of the sol-gel mass takes place in three-stages. The first stage, from 17 °C to 53 °C, where the evaporation of water and solvent leads to a significant weight loss in sol-gel. The second stage is characterized by two exothermic peaks between 53 °C and 400 °C. The first exothermic peak starts at 208 °C and finishes at 241 °C. This peak is assigned to the initial combustion of the organic components, mainly residual epoxy rings [61]. The second exothermic peak at 400 °C represents the maximum thermal degradation of sol-gel and corresponds to the degradation of organic chains such as propyl groups [62]. These findings are in line with previous observations on hybrid sol-gels [63–65]. In the third stage (>400 °C), a broad exothermic peak is observed with a weight loss of 66% of the initial weight. This might be the result of the structural decomposition of organic components, which leads to a glass-like material similar to fused silica (SiO_2) [66]. At 790 °C, the weight of sol-gel stabilized at 26%. The low thermal stability of the sol-gel seems beneficial for combustion processes by not affecting the heat transfer to the pellet significantly.

3.3. Characterization of coating by FTIR spectroscopy

The chemical structure of TEOS/GPTMS sol-gel was identified by FTIR spectroscopy. The FTIR spectrum is presented in Fig. 3, where the black stars indicate the position of peaks in the spectrum.

The weak absorption peaks near 1635 and 957 cm^{-1} indicate the presence of Si–OH bonds. The peaks at 881, 1043 and 1083 cm^{-1} are attributed to the stretching vibration of Si–O–Si bonds [67–69]. The presence of these peaks confirms the polycondensation between TEOS and GPTMS in the coating [70]. The weak peaks at 910 cm^{-1} and 1278 cm^{-1} show the presence of the epoxy ring from GPTMS [71–73], which indicates that a part of the epoxy ring was still available for further hydrolysis/polymerization [74]. The weak and broad peak at 795 cm^{-1} corresponds to the Si–C bonds of the CH_3SiO_3 groups on the surface of silica particles. This is caused by the condensation between Si–OH and GPTMS, which explains the increased hydrophobicity of the coating [25].

3.4. Surface morphology and composition

We used SEM-EDS analysis to investigate the effect of storage on the microstructure and composition of the pellets coated with sol-gel. Fig. 4 presents SEM images of each type of coated pellet before and after 1 month of storage with the corresponding EDS maps (square areas a-f) and locations (numbers 1–3). Table 1 presents the elemental composition obtained at the first ROI on each type of pellet. Detailed SEM-EDS analysis for the second ROI of the studied samples is provided in E-supplementary data.

The transparent nature of the sol-gel coating allows the observation of the uneven and cracked surface of the pellet prior storage (Fig. 4). Pellets are known to have pre-existing cracks resulting from the pelletization process or due to damage during transport, handling and storage

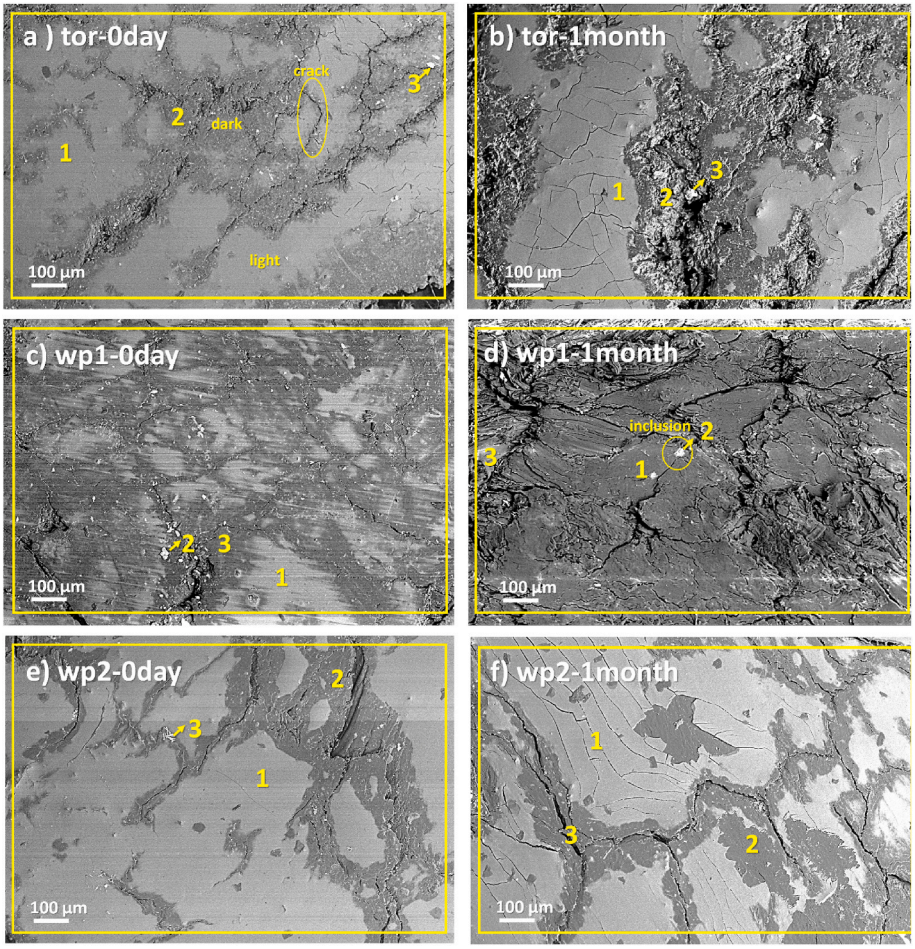

Fig. 4. SEM images of the coated pellets before and after 1 month of storage. **a, b,** tor pellet before (a) and after 1-month storage (b). **c, d,** wp1 pellet before (c) and after 1-month storage (d). **e, f,** wp2 pellet before (e) and after 1-month storage (f). The numbers denote locations where EDS analysis was carried out (Table 1). Areas are denoted by yellow squares and points are denoted by yellow numbers. (For interpretation of the references to color in this figure legend, the reader is referred to the Web version of this article.)

Table 1
Concentrations of elements obtained by EDS analysis at different locations on the surface of the coated pellets shown in Fig. 4, before and after storage.

	Location	C [at. %]	O [at. %]	Si [at. %]	N [at. %]	Mg [at. %]	S [at. %]	P [at. %]	Cl [at. %]	K [at. %]	Ca [at. %]	Mn [at. %]	Fe [at. %]	Cu [at. %]	Zn [at. %]
Fig. 4-a tor-0 day	Area	52.7	38.3	5.6	0.5	0.1	–	–	0.1	0.1	0.2	1.2	1.2	–	–
	1	42.1	43.5	11.1	0.9	–	–	–	–	–	0.1	1.2	1	–	0.1
	2	61.6	31.2	2.8	0.7	–	0.1	–	–	0.2	0.4	1.5	1.5	–	–
	3	48.8	35.1	5.5	0.7	0.1	–	–	0.1	0.1	0.5	1.4	7.7	–	–
Fig. 4-b tor-1 month	Area	48.1	42.4	7.4	0.3	0.1	–	–	0.2	–	0.3	0.4	0.7	0.1	–
	1	39.1	47.7	11.5	0.3	–	–	–	0.3	–	–	0.5	0.5	0.1	–
	2	29.6	44.4	20	0.3	–	–	–	–	–	1.1	2.8	1.8	–	–
	3	63.1	32.3	2.1	1.1	–	0.1	–	–	0.1	0.4	–	0.7	0.1	–
Fig. 4-c wp1-0 day	Area	56.6	37.9	3.6	–	0.1	–	–	0.1	0.1	–	1.5	0.1	–	–
	1	46.3	42.3	7.5	0.2	–	–	–	–	–	–	1.7	1.1	–	–
	2	61.9	32.6	2.8	0.3	0.7	–	–	–	–	–	1.1	0.7	–	–
	3	65.2	30.9	1.9	–	0.1	–	–	–	–	0.1	1	0.6	0.1	0.1
Fig. 4-d wp1-1 month	Area	59.8	39.7	0.2	–	0.1	–	–	–	–	0.1	–	–	0.1	–
	1	67.3	32.5	0.1	–	–	–	–	–	–	0.1	–	–	–	–
	2	42.8	49.3	0.8	–	–	–	–	–	–	6.9	–	0.1	–	0.1
	3	66.6	33.2	–	–	–	–	–	0.1	0.1	–	–	–	–	–
Fig. 4-e wp2-0 day	Area	51.7	38.4	7.6	–	0.1	0.1	–	0.1	–	0.1	0.9	0.9	0.1	–
	1	43.7	42.5	11.8	–	–	–	–	–	–	–	1.4	0.6	–	–
	2	64.6	30.4	2.6	0.3	0.2	–	0.1	–	–	–	1.2	0.6	–	–
	3	45.3	48.2	3	1	–	–	–	–	–	–	0.7	–	0.5	1.3
Fig. 4-f wp2-1 month	Area	49.5	38.9	6.2	–	–	–	–	–	–	–	3.2	2.2	–	–
	1	41.9	45.9	10.9	–	–	–	–	0.1	–	–	0.7	0.5	–	–
	2	65	31.4	2.7	–	–	–	0.1	–	–	–	0.5	0.3	–	–
	3	53.8	40.3	5.4	–	–	–	–	–	–	0.2	–	–	0.2	0.1

[75]. Surface cracks allow media such as moisture to enter into the pellet resulting in reduced structural strength [6]. As can be seen from Fig. 4, the deposition of the coating is more efficient on tor and wp2, which are characterized by a skin-like pattern, compared to wp1 pellets. The skin-like pattern is characterized by light gray areas enriched with Si and O (Table 1), confirming the presence of the coating. On the other hand, dark gray areas indicate that sol-gel was deposited but not homogeneously absorbed by the surface of the pellets. This is supported by EDS experiments reported in our previous research [4], which show that the Si content at the surface of uncoated tor, wp1 and wp2 is 0.48 at %, 0.02 at % and 0.05 at %, respectively. Meanwhile, the darker areas identified on the surface of the coated samples (Fig. 4) have at least one order of magnitude more Si than the uncoated pellets reported in Ref. [4]. The presence of these darker areas has been previously reported when using alkoxysilane-based sol-gel coatings on wood specimens [35].

Furthermore, darker areas with uneven sol-gel absorption rates, especially in wp1, might translate into reduced thickness of the coating layer and less sealing function. This phenomenon is supported by the high visual roughness observed in wp1 (Fig. 4d) and a drop in the Si content after storage compared to before storage conditions (Table 1). In the case of wp1, higher absorption of the coating is expected since this is the most porous pellet of the studied samples with a porosity of 3.6% before coating, as reported in our previous study [4]. These results highlight potential routes for future optimization regarding coating preparation and deposition. Sol-gel should be tailored to the specific physicochemical properties of pellets (elemental composition, porosity and inclusion-to-pellet volume ratio) to prevent deficient deposition or uneven penetration of the coating. Similar phenomena have been observed in coatings used for timber-concrete-composite structures [76].

SEM images also show the presence of inclusions (Fig. 4, bright discernible amorphous particles), mostly at these dark areas, inside or at the border of cracks, where sol-gel was not homogenously absorbed and might lead to higher degradation rates [4].

After 1 month of storage, in general, it is observed that the coating degraded and cracked on all samples due to storage conditions (40 °C and 85% RH) and prolonged storage. The fracture of the coating due to the influence of temperature is in agreement with previous observations using similar coatings over $Ca(OH)_2$ pellets [77]. Yet, the transparency of our coating remained visually unaffected, especially for tor and wp2, which exhibit a protective shield effect after 1 month of storage. These findings are confirmed by EDS analysis, where the concentration of Si on tor (Table 1 b, area, location 1) and wp2 (Table 1 f, area, location 1) remained unchanged after storage compared to before storage conditions (Table 1 a, area, location 1; Table 1 e, area, location 1). With respect to wp1, the concentration of Si before storage is 7.7 at. % (Table 1 c, area, location 1), while 1 month after storage, the Si content decreased to less than 0.2 at. % (Table 1 d, area, location 1). This effect is attributed to the strong bond between the polysiloxane network formed during the sol-gel process and the wood cell wall [23].

Results from the EDS maps (Fig. 4, square yellow areas) suggest that the degradation of the coating might be the result of an oxidation process occurring during storage. After 1 month storage, the concentration of oxygen increased in all pellets (Table 1 b, area; **d**, area and **f**, area). Oxidation of the coating layer might also be one of the reasons for coating cracking after 1 month storage [78]. In humid environments, the cracks in the coating facilitate the diffusion of moisture and oxygen inward the pellet and conversely diffuse the gases from pellet off-gassing [60] outwards through the cracks in the coating. Similar phenomena have been observed in SiC-protected carbon/carbon materials [78].

To evaluate the penetration of the coating, we extracted a 3D profile of the surface of the pellets using digital microscopy. Herein, we used the apparent depth of the cracks as a measure of coating penetration. Pellets with deeper cracks indicate poor sealing protection by the coating, while pellets with small shallow cracks indicate the coating provided an enhanced sealing functionality. Fig. 5 provides the mean apparent depth

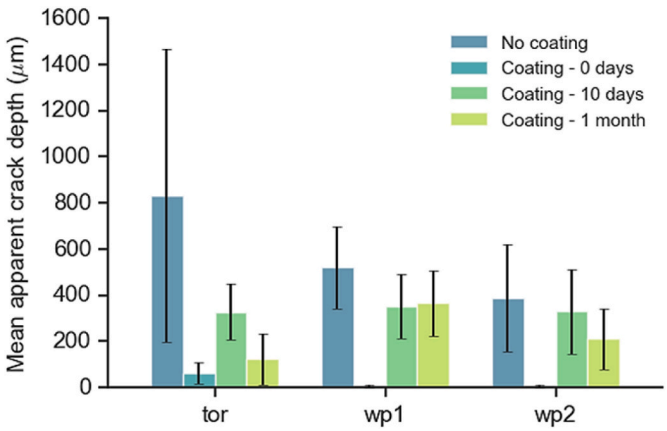

Fig. 5. The mean apparent depth of the cracks observed at the surface of biomass pellets tor, wp1 and wp2 before coating and after coating 0 days, after 10 days and after 1 month of storage. The error bars represent the standard deviation.

of the cracks obtained at the surface of each type of pellet before storage, 10 days after storage and 1 month after storage. Penetration of the coating into the structure of biomass depends on diffusion mechanisms which are strongly related to the surface microstructure and composition of the cell wall [79]. The mean apparent depth of the cracks obtained for all studied samples is given in E-supplementary data.

In general, all uncoated pellets have pre-existing cracks before coating and storage, especially the torrefied ones (Fig. 5, No coating). For example, in some uncoated torrefied samples, cracks extended up to 2.5 mm depth from the surface of the pellets, equivalent to around 40% of the diameter of the pellet. After the pellets were coated and prior storage (Fig. 5, Coating – 0 days), we observed less apparent crack depth, indicating good deposition and penetration of sol-gel coating.

After 10 days of storage, we observed an increase in the apparent crack depth (Fig. 5). This increase is attributed to the degradation of the sol-gel (oxidation) and absorption of sol-gel by the microstructure of biomass [4,80]. This phenomenon is governed by a diffusion process where sol-gel is absorbed by the biomass fibrous structure, allowing the light from the microscope to penetrate into the cracks [4]. After 1 month of storage, the mean apparent crack depth was reduced for all type of pellets compared to 10-days before storage. This is attributed to the extended storage at high humidity which induces plasticization of amorphous polysaccharides in biomass, also referred as softening [79, 81]. The softening facilitates the transport of moisture and minerals through the biomass cell walls leading to swelling and inclusion growth [4,79]. The swelling after 1 month storage is confirmed by diameter measurements (Fig. 1) and findings reported in our previous study [4] for the same type of pellets. After 1 month of storage, coated tor 1 and coated wp2 show major resistance to storage degradation in the form of reduced apparent crack depth compared to conditions prior storage. The mean apparent crack depth in coated tor, coated wp1 and coated wp2 pellets was reduced by 85%, 30% and 46% compared to uncoated conditions.

3.5. *Wettability*

The wettability of each type of pellet was determined by measuring the water contact angles of the coated pellets after different periods of storage (Fig. 6). If the contact angle is smaller than 90°, the surface is hydrophilic and the wettability of the solid is high, while for contact angles larger than 90°, the surface is hydrophobic and the wettability is considered poor [82]. Values of the water contact angle obtained for all studied samples are given in E-supplementary data.

Mean water contact angles for all uncoated pellets are below 44°, which define their hydrophilic character [82]. This is due to biomass

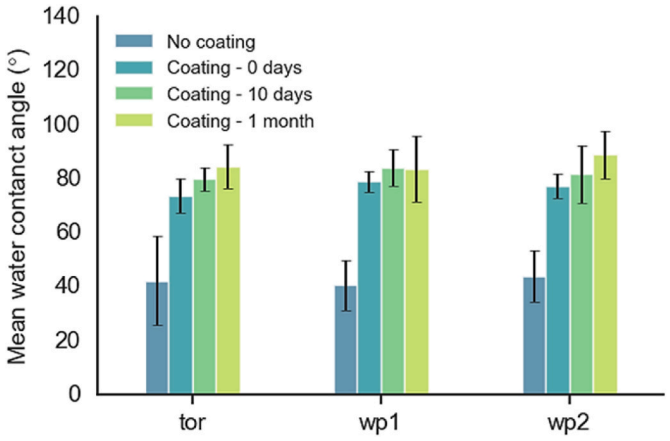

Fig. 6. Mean water contact angles observed at the surface of tor, wp1 and wp2 pellets before coating and after coating at 0 days, 10 days and 1 month after storage. The error bars represent the standard deviation.

pellets have a high concentration of hemicellulose, which is the component of biomass with the highest capacity to adsorb water [83], especially in the untreated ones [7]. We observed large variability in the water contact angle of the torrefied pellets. Results indicate that some uncoated torrefied pellets (tor) have lower wettability than uncoated-untreated pellets. This is mainly because during torrefaction, volatilization and carbonization processes diminish the hemicellulose content of biomass, which makes it less prone to moisture sorption [59, 84].

From Fig. 6 (legend: Coating – 0 days) it is observed that the sol-gel coating decreases substantially the wettability of all coated pellets compared to uncoated ones, regardless of their composition. Thus, these findings represent a pivotal step towards increasing the hydrophobic behavior of biomass pellets. The minimum mean water contact angle (highest wettability) was obtained for coated tor, $74^\circ \pm 6^\circ$. The increased hydrophobicity observed in all coated pellets prior storage is due to successful polymerization between silane precursors within the sol-gel coating. This hypothesis is confirmed by FTIR analysis (Fig. 3).

In extended periods of storage ($\geq$10 days) there seems to be an increase in the interaction between the functional hydroxyl groups of the coating (Fig. 3) and the surrounding moisture [21], which eventually leads to a minor reduction of the coating functionality as shown in SEM images (Fig. 4b, d and f). Nevertheless, the coated pellets remained highly hydrophobic compared to the uncoated ones. This is attributed to the alkoxysilanes in sol-gel, which are known to be hydrophobic and prevent the formation of hydrogen bonds between the coated pellet's surface and moisture [36].

The contact angles for all samples increased proportionally to the storage time. After 1 month of storage, we obtained the highest hydrophobic response for all the samples and experimental conditions. This might be attributed to a swelling mechanism (Figs. 1 and 5) which leads to fewer cracks at the pellet's surface, which in turn results in less media penetrating the pellet and decreased wettability [4,30]. It is known that the wettability of solid surfaces is highly influenced by the microstructure topography, where higher surface roughness usually leads to higher contact angle [21]. Evidence provided by Ref. [21] using atomic force microscopy indicates that sol-gel coatings applied to solid surfaces tend to produce "islands/patches" with increased height at the coating surface, leading to high water contact angles. The increased contact angles after 1 month storage confirm the positive effect of our sol-gel as a protection for pellets to endure indoor storage degradation and likely to resist outdoor storage.

4. Conclusions

We show that using a GPTMS/TEOS hybrid sol-gel as a surface treatment can result in durable biomass pellets that can tolerate storage degradation even at relatively high ambient temperature and humidity conditions. After 1 month storage, the coating decreased the wettability of all pellets by 103% on average when compared to the uncoated ones. The important finding from this work is related to torrefied pellets. After sol-gel deposition, coated untreated pellets have lower wettability than non-coated torrefied pellets, which for some applications might provide a cost-competitive alternative to torrefaction. Especially for applications that can counterweigh the increased grindability and energy density of the torrefied material with more durable coated untreated pellets.

E-supplementary data of this work can be found in the online version of the paper.

CRediT authorship contribution statement

Luis Cutz: Conceptualization, Methodology, Investigation, Validation, Writing – original draft, Visualization. **Urša Tiringer:** Conceptualization, Methodology, Investigation, Validation, Writing – original draft, Visualization. **Wiebren de Jong:** Writing – review & editing, Supervision. **Arjan Mol:** Writing – review & editing, Supervision.

Declaration of competing interest

The authors declare that they have no known competing financial interests or personal relationships that could have appeared to influence the work reported in this paper.

Data availability

Data will be made available on request.

Acknowledgements

This work was supported by the Top Consortium for Knowledge and Innovation for the Biobased Economy under grant TKI-BBE project number BBE-1801. Additional support was provided by the European Union's Horizon 2020 research and innovation programme under the Marie Skłodowska-Curie grant agreement No. 707404.

Appendix A. Supplementary data

Supplementary data to this article can be found online at https://doi.org/10.1016/j.matchemphys.2023.127861.

References

[1] C. Calderón, M. Colla, J.M. Jossart, N. Hemeleers, A. Martin, N. Aveni, C. Caferri, Statistical Report 2019: Report Pellet, BIOENERGY EUROPE, 2019.
[2] F. Yazdanpanah, S. Sokhansanj, A.K. Lau, C.J. Lim, X. Bi, S. Melin, M. Afzal, Permeability of wood pellets in the presence of fines, Bioresour. Technol. 101 (2010) 5565–5570, https://doi.org/10.1016/j.biortech.2010.01.096.
[3] E. Alakoski, M. Jämsén, D. Agar, E. Tampio, M. Wihersaari, From wood pellets to wood chips, risks of degradation and emissions from the storage of woody biomass – a short review, Renew. Sustain. Energy Rev. 54 (2016) 376–383, https://doi.org/10.1016/j.rser.2015.10.021.
[4] L. Cutz, U. Tiringer, H. Gilvari, D. Schott, A. Mol, W. de Jong, Microstructural degradation during the storage of biomass pellets, Communications Materials 2 (2021) 1–12, https://doi.org/10.1038/s43246-020-00113-y.
[5] D. Ilic, K. Williams, R. Farnish, E. Webb, G. Liu, On the challenges facing the handling of solid biomass feedstocks, Biofuels, Bioproducts and Biorefining 12 (2018) 187–202, https://doi.org/10.1002/bbb.1851.
[6] T. Deng, A.M. Alzahrani, M.S. Bradley, Influences of environmental humidity on physical properties and attrition of wood pellets, Fuel Process. Technol. 185 (2019) 126–138, https://doi.org/10.1016/j.fuproc.2018.12.010.
[7] H. Gilvari, L. Cutz, U. Tiringer, A. Mol, W. de Jong, D.L. Schott, The effect of environmental conditions on the degradation behavior of biomass pellets, Polymers 12 (2020) 970, https://doi.org/10.3390/polym12040970.

[8] J.S. Lee, S. Sokhansanj, A.K. Lau, J. Lim, X.T. Bi, Moisture adsorption rate and durability of commercial softwood pellets in a humid environment, Biosyst. Eng. 203 (2021) 1–8, https://doi.org/10.1016/j.biosystemseng.2020.12.011.
[9] V. Schlünssen, A.M. Madsen, S. Skov, T. Sigsgaard, Does the use of biofuels affect respiratory health among male Danish energy plant workers? Occup. Environ. Med. 68 (2011) 467–473, https://doi.org/10.1136/oem.2009.054403.
[10] J. Berghel, S. Frodeson, K. Granström, R. Renström, M. Ståhl, D. Nordgren, P. Tomani, The effects of kraft lignin additives on wood fuel pellet quality, energy use and shelf life, Fuel Process. Technol. 112 (2013) 64–69, https://doi.org/10.1016/j.fuproc.2013.02.011.
[11] D. Tarasov, C. Shahi, M. Leitch, Effect of Additives on Wood Pellet Physical and Thermal Characteristics: A Review, International Scholarly Research Notices, 2013, https://doi.org/10.1155/2013/876939.
[12] H.S. Kambo, A. Dutta, Strength, storage, and combustion characteristics of densified lignocellulosic biomass produced via torrefaction and hydrothermal carbonization, Appl. Energy 135 (2014) 182–191, https://doi.org/10.1016/j.apenergy.2014.08.094.
[13] J.S. Tumuluru, Effect of deep drying and torrefaction temperature on proximate, ultimate composition, and heating value of 2-mm lodgepole pine (Pinus contorta) grind, Bioengineering 3 (2016), https://doi.org/10.3390/bioengineering3020016.
[14] M. Tan, L. Luo, Z. Wu, Z. Huang, J. Zhang, J. Huang, Y. Yang, X. Zhang, H. Li, Pelletization of Camellia oleifera Abel. shell after storage: energy consumption and pellet properties, Fuel Process. Technol. 201 (2020), 106337, https://doi.org/10.1016/j.fuproc.2020.106337.
[15] I. Yang, M. Cooke-Willis, B. Song, P. Hall, Densification of torrefied Pinus radiata sawdust as a solid biofuel: effect of key variables on the durability and hydrophobicity of briquettes, Fuel Process. Technol. 214 (2021), 106719, https://doi.org/10.1016/j.fuproc.2020.106719.
[16] R.R. Myers, History of coatings science and technology, J. Macromol. Sci. Part A - Chemistry 15 (1981) 1133–1149, https://doi.org/10.1080/00222338108066457.
[17] M. Guglielmi, Sol-gel coatings on metals, J. Sol. Gel Sci. Technol. 8 (1997) 443–449, https://doi.org/10.1007/BF02436880.
[18] C. Carrera-Figueiras, Y. Pérez-Padilla, M.A. Estrella-Gutiérrez, E.G. Uc-Cayetano, J. A. Juárez-Moreno, A. Avila-Ortega, Surface Science Engineering through Sol-Gel Process, IntechOpen, 2019, https://doi.org/10.5772/intechopen.83676.
[19] J.M. Craven, J. Swithenbank, V.N. Sharifi, D. Peralta-Solorio, G. Kelsall, P. Sage, Hydrophobic coatings for moisture stable wood pellets, Biomass Bioenergy 80 (2015) 278–285, https://doi.org/10.1016/j.biombioe.2015.06.004.
[20] A. Tilay, R. Azargohar, M. Drisdelle, A. Dalai, J. Kozinski, Canola meal moisture-resistant fuel pellets: study on the effects of process variables and additives on the pellet quality and compression characteristics, Ind. Crop. Prod. 63 (2015) 337–348, https://doi.org/10.1016/j.indcrop.2014.10.008.
[21] A. Venkateswara Rao, S.S. Latthe, D.Y. Nadargi, H. Hirashima, V. Ganesan, Preparation of MTMS based transparent superhydrophobic silica films by sol–gel method, J. Colloid Interface Sci. 332 (2009) 484–490, https://doi.org/10.1016/j.jcis.2009.01.012.
[22] H. Chang, K. Tu, X. Wang, J. Liu, Fabrication of mechanically durable superhydrophobic wood surfaces using polydimethylsiloxane and silica nanoparticles, RSC Adv. 5 (2015) 30647–30653, https://doi.org/10.1039/C5RA03070F.
[23] M.A. Tshabalala, J.E. Gangstad, Accelerated weathering of wood surfaces coated with multifunctional alkoxysilanes by sol-gel deposition, J. Coating Technol. 75 (2003) 37–43, https://doi.org/10.1007/BF02730098.
[24] M.A. Tshabalala, L.-P. Sung, Wood surface modification by in-situ sol-gel deposition of hybrid inorganic-organic thin films, J. Coating Technol. Res. 4 (4) (2007) [8] Pages. (2007, https://www.fs.usda.gov/treesearch/pubs/32709. (Accessed 13 October 2020).
[25] S.S. Latthe, H. Imai, V. Ganesan, A. Venkateswara Rao, Porous superhydrophobic silica films by sol–gel process, Microporous Mesoporous Mater. 130 (2010) 115–121, https://doi.org/10.1016/j.micromeso.2009.10.020.
[26] F. Girardi, E. Cappelletto, J. Sandak, G. Bochicchio, B. Tessadri, S. Palanti, E. Feci, R. Di Maggio, Hybrid organic–inorganic materials as coatings for protecting wood, Prog. Org. Coating 77 (2014) 449–457, https://doi.org/10.1016/j.porgcoat.2013.11.010.
[27] C.J. Brinker, A.J. Hurd, P.R. Schunk, G.C. Frye, C.S. Ashley, Review of sol-gel thin film formation, J. Non-Cryst. Solids 147–148 (1992) 424–436, https://doi.org/10.1016/S0022-3093(05)80653-2.
[28] R.B. Figueira, Hybrid sol–gel coatings for corrosion mitigation: a critical review, Polymers 12 (2020) 689, https://doi.org/10.3390/polym12030689.
[29] V.B. Kandimalla, V.S. Tripathi, H. Ju, Chapter 16 - biosensors based on immobilization of biomolecules in sol-gel matrices, in: X. Zhang, H. Ju, J. Wang (Eds.), Electrochemical Sensors, Biosensors and Their Biomedical Applications, Academic Press, San Diego, 2008, pp. 503–529, https://doi.org/10.1016/B978-012373738-0.50018-0.
[30] L. Qu, S. Rahimi, J. Qian, L. He, Z. He, S. Yi, Preparation and characterization of hydrophobic coatings on wood surfaces by a sol-gel method and post-aging heat treatment, Polym. Degrad. Stabil. 183 (2021), 109429, https://doi.org/10.1016/j.polymdegradstab.2020.109429.
[31] D. Balgude, A. Sabnis, Sol–gel derived hybrid coatings as an environment friendly surface treatment for corrosion protection of metals and their alloys, J. Sol. Gel Sci. Technol. 64 (2012) 124–134, https://doi.org/10.1007/s10971-012-2838-z.
[32] R. Ciriminna, M. Pagliaro, Silica-based sol-gel microencapsulation and applications, in: Handbook of Encapsulation and Controlled Release, Munmaya Mishra, CRC Press, 2016, p. 344. https://www.routledge.com/Handbook-of-Encapsulation-and-Controlled-Release/Mishra/p/book/9781482232325. (Accessed 2 February 2022).
[33] D. Chen, Anti-reflection (AR) coatings made by sol–gel processes: a review, Sol. Energy Mater. Sol. Cell. 68 (2001) 313–336, https://doi.org/10.1016/S0927-0248(00)00365-2.
[34] R.B. Figueira, I.R. Fontinha, C.J.R. Silva, E.V. Pereira, Hybrid sol-gel coatings: smart and green materials for corrosion mitigation, Coatings 6 (2016) 12, https://doi.org/10.3390/coatings6010012.
[35] A.-C. Ristschkoff, R. Mahlberg, M. Löija, M. Kallio, et al., Sol-gel hybrid coatings for wood products with improved surface durability and repellence properties, Paint Coating Ind. 21 (96–98) (2005) 100–101.
[36] M.A. Tshabalala, P. Kingshott, M.R. VanLandingham, D. Plackett, Surface chemistry and moisture sorption properties of wood coated with multifunctional alkoxysilanes by sol-gel process, J. Appl. Polym. Sci. 88 (2003) 2828–2841, 2003, https://www.fs.usda.gov/treesearch/pubs/8579. (Accessed 3 December 2020).
[37] C.J. Brinker, Sol-Gel Science, first ed., 1990. https://www.elsevier.com/books/sol-gel-science/brinker/978-0-08-057103-4. (Accessed 18 April 2022).
[38] R.B. Figueira, C.J.R. Silva, E.V. Pereira, Organic–inorganic hybrid sol–gel coatings for metal corrosion protection: a review of recent progress, J. Coating Technol. Res. 12 (2015) 1–35, https://doi.org/10.1007/s11998-014-9595-6.
[39] I. Izarra, J. Cubillo, A. Serrano, J.F. Rodriguez, M. Carmona, A hydrophobic release agent containing SiO2-CH3 submicron-sized particles for waterproofing mortar structures, Construct. Build. Mater. 199 (2019) 30–39, https://doi.org/10.1016/j.conbuildmat.2018.12.018.
[40] Z. Sun, B. Liu, S. Huang, J. Wu, Q. Zhang, Facile fabrication of superhydrophobic coating based on polysiloxane emulsion, Prog. Org. Coating 102 (2017) 131–137, https://doi.org/10.1016/j.porgcoat.2016.07.003.
[41] K. Tu, X. Wang, L. Kong, H. Guan, Facile preparation of mechanically durable, self-healing and multifunctional superhydrophobic surfaces on solid wood, Mater. Des. 140 (2018) 30–36, https://doi.org/10.1016/j.matdes.2017.11.029.
[42] X. Zhao, Y. Li, B. Li, T. Hu, Y. Yang, L. Li, J. Zhang, Environmentally benign and durable superhydrophobic coatings based on SiO2 nanoparticles and silanes, J. Colloid Interface Sci. 542 (2019) 8–14, https://doi.org/10.1016/j.jcis.2019.01.115.
[43] C. Di Blasi, Modeling chemical and physical processes of wood and biomass pyrolysis, Prog. Energy Combust. Sci. 34 (2008) 47–90, https://doi.org/10.1016/j.pecs.2006.12.001.
[44] M.-C. Popescu, C.-M. Popescu, G. Lisa, Y. Sakata, Evaluation of morphological and chemical aspects of different wood species by spectroscopy and thermal methods, J. Mol. Struct. 988 (2011) 65–72, https://doi.org/10.1016/j.molstruc.2010.12.004.
[45] C. Huang, C.-H. Liu, C.-H. Su, W.-T. Hsu, S.-Y. Wu, Investigation of atmospheric-pressure plasma deposited SiOx films on polymeric substrates, Thin Solid Films 517 (2009) 5141–5145, https://doi.org/10.1016/j.tsf.2009.03.054.
[46] C. Mai, H. Militz, Modification of wood with silicon compounds. Treatment systems based on organic silicon compounds — a review, Wood Sci. Technol. 37 (2004) 453–461, https://doi.org/10.1007/s00226-004-0225-9.
[47] Y.-C. Sheen, W.-H. Chang, W.-C. Chen, Y.-H. Chang, Y.-C. Huang, F.-C. Chang, Non-fluorinated superamphiphobic surfaces through sol–gel processing of methyltriethoxysilane and tetraethoxysilane, Mater. Chem. Phys. 114 (2009) 63–68, https://doi.org/10.1016/j.matchemphys.2008.07.132.
[48] G.-L. Xu, L.-L. Deng, P.-H. Pi, X.-F. Wen, D.-F. Zhen, Z.-Q. Cai, Q. Chen, Z.-R. Yang, Preparation and characterization of superhydrophobic/superoleophilic SiO2 film, Integrated Ferroelectrics Int. J. 127 (2011) 9–14, https://doi.org/10.1080/10584587.2011.575274.
[49] E. Pargoletti, L. Motta, V. Comite, P. Fermo, G. Cappelletti, The hydrophobicity modulation of glass and marble materials by different Si-based coatings, Prog. Org. Coating 136 (2019), 105260, https://doi.org/10.1016/j.porgcoat.2019.105260.
[50] O.-H. Park, Y.-J. Eo, Y.-K. Choi, B.-S. Bae, Preparation and optical properties of silica-poly(ethylene oxide) hybrid materials, J. Sol. Gel Sci. Technol. 16 (1999) 235–241, https://doi.org/10.1023/A:1008717219952.
[51] C. Schramm, W.H. Binder, R. Tessadri, Durable press finishing of cotton fabric with 1,2,3,4-butanetetracarboxylic acid and TEOS/GPTMS, J. Sol. Gel Sci. Technol. 29 (2004) 155–165, https://doi.org/10.1023/B:JSST.0000023850.97771.7d.
[52] U. Tiringer, I. Milošev, A. Durán, Y. Castro, Hybrid sol–gel coatings based on GPTMS/TEOS containing colloidal SiO2 and cerium nitrate for increasing corrosion protection of aluminium alloy 7075-T6, J. Sol. Gel Sci. Technol. (2018), https://doi.org/10.1007/s10971-017-4577-7.
[53] W.D. Lee, R. Gawri, R.M. Pilliar, W.L. Stanford, R.A. Kandel, Sol gel-derived hydroxyapatite films over porous calcium polyphosphate substrates for improved tissue engineering of osteochondral-like constructs, Acta Biomater. 62 (2017) 352–361, https://doi.org/10.1016/j.actbio.2017.08.016.
[54] U. Tiringer, J.P.B. van Dam, S.T. Abrahami, H. Terryn, J. Kovač, I. Milošev, J.M. C. Mol, Scrutinizing the importance of surface chemistry versus surface roughness for aluminium/sol-gel film adhesion, Surface. Interfac. 26 (2021), 101417, https://doi.org/10.1016/j.surfin.2021.101417.
[55] J. Lee, S. Sokhansanj, A.P.T. Lau, C.J. Lim, X. Bi, V. Basset, F. Yazdanpanah, S. Melin, The effects of storage on the net calorific value of wood pellets. https://doi.org/10.7451/CBE.2015.57.8.5, 2015.
[56] S. Wang, X. Yuan, C. Li, Z. Huang, L. Leng, G. Zeng, H. Li, Variation in the physical properties of wood pellets and emission of aldehyde/ketone under different storage conditions, Fuel 183 (2016) 314–321, https://doi.org/10.1016/j.fuel.2016.06.083.
[57] KEYENCE, Digital Microscope VHX-5000. User's Manual, KEYENCE CORPORATION, Japan, 2014.
[58] J. Shankar Tumuluru, S. Sokhansanj, J.R. Hess, C.T. Wright, R.D. Boardman, REVIEW: a review on biomass torrefaction process and product properties for

energy applications, Ind. Biotechnol. 7 (2011) 384–401, https://doi.org/10.1089/ind.2011.7.384.
[59] Y. Zhang, F. Chen, D. Chen, K. Cen, J. Zhang, X. Cao, Upgrading of Biomass Pellets by Torrefaction and its Influence on the Hydrophobicity, Mechanical Property, and Fuel Quality, Biomass Conv. Bioref., 2020, https://doi.org/10.1007/s13399-020-00666-5.
[60] Y. Xi, X. Yuan, M. Tan, S. Jiang, Z. Wang, Z. Huang, H. Wang, L. Jiang, H. Li, Properties of oxidatively torrefied Chinese fir residue: color dimension, pyrolysis kinetics, and storage behavior, Fuel Process. Technol. 213 (2021), 106663, https://doi.org/10.1016/j.fuproc.2020.106663.
[61] J. Mosa, A. Durán, M. Aparicio, Proton conducting sol–gel sulfonated membranes produced from 2-allylphenol, 3-glycidoxypropyl trimethoxysilane and tetraethyl orthosilicate, J. Power Sources 192 (2009) 138–143, https://doi.org/10.1016/j.jpowsour.2008.12.126.
[62] J. Mosa, A. Durán, M. Aparicio, Epoxy-polystyrene-silica sol–gel membranes with high proton conductivity by combination of sulfonation and tungstophosphoric acid doping, J. Membr. Sci. 361 (2010) 135–142, https://doi.org/10.1016/j.memsci.2010.05.063.
[63] M. Hernández-Escolano, X. Ramis, A. Jiménez-Morales, M. Juan-Díaz, J. Suay, Study of the thermal degradation of bioactive sol–gel coatings for the optimization of its curing process, J. Therm. Anal. Calorim. 107 (2012) 499–508, https://doi.org/10.1007/s10973-011-1553-2.
[64] D. Li, F. Xu, L. Shao, M. Wang, Effect of the addition of 3-glycidoxypropyltrimethoxysilane to tetraethoxyorthosilicate-based stone protective coating using n-octylamine as a catalyst, Bull. Mater. Sci. 38 (2015) 49–55, https://doi.org/10.1007/s12034-014-0795-6.
[65] A. Suarez Vega, C. Agustín-Sáenz, F. Brusciotti, A. Somers, M. Forsyth, Effect of lanthanum 4-hydroxy cinnamate on the polymerisation, condensation and thermal stability of hybrid sol–gel formulations, J. Sol. Gel Sci. Technol. 96 (2020) 91–107, https://doi.org/10.1007/s10971-020-05315-x.
[66] M. Zaharescu, L. Predoana, J. Pandele, Relevance of thermal analysis for sol–gel-derived nanomaterials, J. Sol. Gel Sci. Technol. 86 (2018) 7–23, https://doi.org/10.1007/s10971-018-4583-4.
[67] M. Catauro, F. Bollino, F. Papale, M. Gallicchio, S. Pacifico, Synthesis and chemical characterization of new silica polyethylene glycol hybrid nanocomposite materials for controlled drug delivery, J. Drug Deliv. Sci. Technol. 24 (2014) 320–325, https://doi.org/10.1016/S1773-2247(14)50069-X.
[68] M. Criado, I. Sobrados, J. Sanz, Polymerization of hybrid organic–inorganic materials from several silicon compounds followed by TGA/DTA, FTIR and NMR techniques, Prog. Org. Coating 77 (2014) 880–891, https://doi.org/10.1016/j.porgcoat.2014.01.019.
[69] F. Shams-Ghahfarokhi, A. Khoddami, Z. Mazrouei-Sebdani, J. Rahmatinejad, H. Mohammadi, A new technique to prepare a hydrophobic and thermal insulating polyester woven fabric using electro-spraying of nano-porous silica powder, Surf. Coating. Technol. 366 (2019) 97–105, https://doi.org/10.1016/j.surfcoat.2019.03.025.
[70] U. Tiringer, A. Durán, Y. Castro, I. Milošev, Self-Healing effect of hybrid sol-gel coatings based on GPTMS, TEOS, SiO2 nanoparticles and Ce(NO3)3 applied on aluminum alloy 7075-T6, J. Electrochem. Soc. 165 (2018) C213, https://doi.org/10.1149/2.0211805jes.
[71] A.J. Vreugdenhil, V.N. Balbyshev, M.S. Donley, Nanostructured silicon sol-gel surface treatments for Al 2024-T3 protection, J. Coating Technol. 73 (2001) 35–43, https://doi.org/10.1007/BF02730029.
[72] X. Zhong, Q. Li, J. Hu, X. Yang, F. Luo, Y. Dai, Effect of cerium concentration on microstructure, morphology and corrosion resistance of cerium–silica hybrid coatings on magnesium alloy AZ91D, Prog. Org. Coating 69 (2010) 52–56, https://doi.org/10.1016/j.porgcoat.2010.05.004.
[73] R. Zandi-zand, A. Ershad-langroudi, A. Rahimi, Silica based organic–inorganic hybrid nanocomposite coatings for corrosion protection, Prog. Org. Coating 53 (2005) 286–291, https://doi.org/10.1016/j.porgcoat.2005.03.009.
[74] S.-M. Shang, Z. Li, Y. Xing, J.H. Xin, X.-M. Tao, Preparation of durable hydrophobic cellulose fabric from water glass and mixed organosilanes, Appl. Surf. Sci. 257 (2010) 1495–1499, https://doi.org/10.1016/j.apsusc.2010.08.081.
[75] W. Stelte, J.K. Holm, A.R. Sanadi, S. Barsberg, J. Ahrenfeldt, U.B. Henriksen, A study of bonding and failure mechanisms in fuel pellets from different biomass resources, Biomass Bioenergy 35 (2011) 910–918, https://doi.org/10.1016/j.biombioe.2010.11.003.
[76] M. Brunner, M. Romer, M. Schnüriger, Timber-concrete-composite with an adhesive connector (wet on wet process), Mater. Struct. 40 (2007) 119–126, https://doi.org/10.1617/s11527-006-9154-4.
[77] L. Briones, C.M. Valverde-Pizarro, I. Barras-García, C. Tajuelo, E.S. Sanz-Pérez, R. Sanz, J.M. Escola, J. González-Aguilar, M. Romero, Development of stable porous silica-coated Ca(OH)2/γ-Al2O3 pellets for dehydration/hydration cycles with application in thermochemical heat storage, J. Energy Storage 51 (2022), 104548, https://doi.org/10.1016/j.est.2022.104548.
[78] N.S. Jacobson, D.J. Roth, R.W. Rauser, J.D. Cawley, D.M. Curry, Oxidation through coating cracks of SiC-protected carbon/carbon, Surf. Coating. Technol. 203 (2008) 372–383, https://doi.org/10.1016/j.surfcoat.2008.09.013.
[79] J.E. Jakes, Mechanism for diffusion through secondary cell walls in lignocellulosic biomass, 123, J. Phys. Chem. B 123 (19) (2019) 4333–4339, https://doi.org/10.1021/acs.jpcb.9b01430, 4333–4339.
[80] J.E. Jakes, C.G. Hunt, S.L. Zelinka, P.N. Ciesielski, N.Z. Plaza, Effects of moisture on diffusion in unmodified wood cell walls: a phenomenological polymer science approach, Forests 10 (2019) 1084, https://doi.org/10.3390/f10121084.
[81] J.S. Vrentas, C.M. Vrentas, Sorption in glassy polymers, Macromolecules 24 (1991) 2404–2412, https://doi.org/10.1021/ma00009a043.
[82] W.-H. Chen, B.-J. Lin, B. Colin, A. Pétrissans, M. Pétrissans, A study of hygroscopic property of biomass pretreated by torrefaction, Energy Proc. 158 (2019) 32–36, https://doi.org/10.1016/j.egypro.2019.01.030.
[83] T.C. Acharjee, C.J. Coronella, V.R. Vasquez, Effect of thermal pretreatment on equilibrium moisture content of lignocellulosic biomass, Bioresour. Technol. 102 (2011) 4849–4854, https://doi.org/10.1016/j.biortech.2011.01.018.
[84] N. Setkit, X. Li, H. Yao, N. Worasuwannarak, Torrefaction behavior of hot-pressed pellets prepared from leucaena wood, Bioresour. Technol. 321 (2021), 124502, https://doi.org/10.1016/j.biortech.2020.124502.